Temporal Variability in the Impacts of Particulate Matter on Crop Yields on the North China Plain

Authors: Michael Wolffe[a] (Corresponding author), Oliver Wild[a], Stephen Long[ab], Kirsti Ashworth[a]

[a] Lancaster Environment Centre, Lancaster University, Bailrigg, Lancaster, LA1 4YW, United Kingdom

[b] Crop Sciences and Plant Biology, University of Illinois at Urbana-Champaign, 1206 W Gregory Dr, Urbana, IL 61801, United States

Author Contributions

Michael Wolffe: Conceptualization, Methodology, Software, Validation, Formal Analysis, Investigation, Data Curation, Writing – Original Draft, Writing – Review & Editing, Visualisation, Project Administration.
Oliver Wild: Conceptualization, Methodology, Supervision, Writing – Review & Editing. **Stephen Long:** Conceptualization, Supervision, Writing – Review & Editing. **Kirsti Ashworth:** Conceptualization, Methodology, Resources, Writing – Review & Editing, Supervision, Project Administration, Funding Acquisition.

Abstract

The North China Plain (NCP) is a major agricultural region, producing 45% of China's maize. It is also vital to the Chinese economy, encompassing the Beijing-Tianjin-Hebei megacity region. Anthropogenic factors increasingly impact crop yields on the NCP, and globally. Particulate matter (PM) pollution is a significant problem in this region, where annual average PM concentrations over three times the Chinese national air quality standard were recorded for the Beijing-Tianjin-Hebei megacity region between 2013-18. PM absorbs light, reducing total shortwave radiation (SW), thereby limiting plant productivity. However, PM also scatters incoming SW, increasing the diffuse fraction, which has been shown to increase growth and biomass assimilation.

27

28   The Joint UK Land Environment Simulator (JULES) crop model was used to assess the net impact of

29   these competing changes in light on NCP maize yields. In contrast to some previous analyses, we find

30   that PM-associated decreases in SW outweigh any positive impact on yield from an increasing proportion

31   of diffuse radiation.

32

33   Furthermore, carbon allocation to different portions of the growing cropchanges during the development

34   cycle. We find significant differences between the effect on final yield of identical changes to diffuse

35   fraction and total SW occurring during different development stages. The greatest simulated yield gains

36   from increased SW and reduced diffuse fraction, consistent with reductions in PM, are observed during

37   the early reproductive stage of development (July-August), when the simulated gain of yield is as much

38   as 12.9% more than in other periods.

39

40   To further assess the impact of PM-linked changes in SW and diffuse fraction on NCP crop yields,

41   radiation profiles from different city regions were then applied across the NCP. The changes in SW

42   associated with these city regions could increase maize yields across China by ~8 Mt. This would

43   completely offset China's annual maize imports, increasing both national and global food security.

44

45   1. Introduction

46   The North China Plain (NCP) is China's largest agricultural region, accounting for 61% of the country's

47   wheat and 45% of its maize production (Yang *et al*. 2015). Today China is a major importer of wheat and

48   maize (FAOSTAT, 2020). Increasing production in the NCP is therefore not only important for local farm

49   economies, but also in reducing pressures on world grain markets. Maize production has risen twelvefold

50   in the NCP over the last 6 decades(Li, 2009) and maize now comprises China's most important feedstock

51   for livestock production (Shihuang and Kaijian, 2010).

52

53   Since the 1980s, climate change has begun to impact maize and wheat yields due to rising average

54   temperature, only ameliorated by adoption of new crop varieties and better agronomic practices by

55   producers (Liu YA *et al*., 2010, Han D. *et al*. 2018). The NCP includes the megacity region of Beijing-

56 Tianjin-Hebei. Air pollution resulting from transportation, energy generation and industry in these major

57 populations centres is known to affect crop yields (Feng et al., 2015; Masutomi et al., 2018). One

58 important component of air pollution is particulate matter (PM), which persists at high concentrations over

59 the NCP. Annual average concentrations of PM2.5, i.e. particles with diameter ≤ 2.5 µm, of 108 ± 34 µg

60 m^{-3} were recorded in Beijing-Tianjin-Hebei for 2013-18 (Zhai et al., 2019). This far exceeds the

61 international and national air quality guidelines for an average mean concentration of 10 µg/m^{-3} (WHO,

62 2015) and 35 µg/m^{-3} (China: Air Quality Standards | Transport Policy, 2013) respectively. Such high

63 levels of PM2.5 strongly affect both the intensity of short-wave (SW) radiation and the ratio of diffuse to

64 direct SW radiation reaching the Earth's surface. PM occurs at high concentrations, not just in the NCP,

65 but in many key crop growing regions around the world, particularly in developing nations. For example,

66 the Indo-Gangetic Plain produces ~50% of India's food (Dhillon *et al*, 2010, Timsina J, 2012). However,

67 PM pollution in this region can reach 100 µg m^{-3} (Ojha N., *et al.* 2020), and is predicted to significantly

68 reduce crop yields (Mina U. *et al.* 2018). The global nature of PM pollution, and its ubiquity and increase

69 in key areas of global crop production has implications for global food security, making it critical to better

70 quantify its impacts on crop yields.

71

72 PM is a heterogeneous mix of airborne particles, with highly variable chemical and physical properties.

73 The particle composition, size distribution and altitude of aerosol govern how it interacts with SW

74 radiation. For example, highly light absorbing particles, such as soot and black carbon from combustion of

75 coal for heat in the winter, directly reduce total SW levels at the Earth's surface (Moosmüller, Chakrabarty

76 and Arnott, 2009; Cohan *et al.*, 2002).

77

78 For well managed and watered crops, there is a linear relationship between absorbed SW radiation and

79 crop biomass accumulation (Monteith, 1977; Dohleman & Long, 2009); any reduction in incoming SW will

80 therefore lower production. Reductions, such as those caused by PM, are exacerbated in so-called haze

81 events, where atmospheric inversion results in an accumulation of pollutant at low altitude, strongly

82 reducing surface SW (Aziz *et al.*, 2019). Such haze events are a key cause of reduced visibility and

83 surface SW in the North China Plains (Z. An *et al.*, 2019; Han *et al.*, 2012; Guo *et al.*, 2014). Although

84 most common in December and January, 5-6 haze days per month are also observed from April to

85 September, the main period of maize production (Chen & Wang, 2015).

87 Other PM aerosol components such as sulphate are more reflective (Ramanathan *et al.*, 2001),

88 scattering light instead of absorbing it. Intercepted light may be scattered in all directions by PM, both

89 reducing SW reaching the surface and altering its angular distribution, increasing the proportion which is

90 diffuse (Huang *et al.*, 2014). Well-managed crops will typically form about a dense canopy of 5-7 m^2 of

91 leaves per m^2 of ground. Direct beam sunlight is therefore largely intercepted by the uppermost leaves of

92 crop plants, with most leaves below in shade (Wickens and Horn, 1972). In full sunlight, upper leaves

93 intercept more light than they can use in photosynthesis, while photosynthesis is light-limited in the lower

94 canopy (Ort et al. 2015). Diffuse SW reaches the surface from all angles of the hemisphere, enabling it

95 to penetrate deeper into crop canopies and allowing increased photosynthesis by the light-limited lower

96 leaves. This more even distribution of radiation through the canopy under high levels of diffuse light

97 reduces the risk of oversaturation and thus photo-inhibition in the upper canopy. This redistribution of light

98 to other canopy layers increases radiation use efficiency (RUE) for the plant overall, improving the rates

99 of carbon fixation, net canopy photosynthesis, and hence, gross primary production (GPP) in forest

100 ecosystems (Roderick *et al.*, 2001; Niyogi *et al.*, 2004; Kanniah *et al.*, 2012; Rap *et al.*, 2015) and is

101 known as "diffuse light fertilisation" (Gu *et al.*, 2002).

102

103 Variations in PM composition mean that changes in PM concentration do not strictly map to changes in

104 surface radiation. This is compounded by variations in PM size distribution and meteorology which further

105 affect how PM interacts with incoming radiation. Evidence for this can be seen in the widely fluctuating

106 PM concentration over the year on the NCP. As PM concentration increases during the winter and

107 declines in the summer, one would perhaps expect a relatively simple relationship where increased PM

108 concentration directly maps to reduced radiation intensity at the earth's surface. However, aerosol optical

109 depth (AOD), a key measure of the impact of total column aerosol on incoming radiation, peaks instead in

110 late summer (Qu, Wang, Zhang, Sheng, & Wang, 2016) due to the prevailing meteorological conditions at

111 that time of year. Furthermore in winter, PM composition becomes increasingly black and organic carbon

112 heavy, as combustion based power stations increasingly burn coal to provide heating during the winter

113 months. This provides a marked difference in PM composition profile to the summer months when highly

114 reflective nitrate aerosols dominate (Qu, Wang, Zhang, Sheng, & Wang, 2016), leading to different

115 impacts on surface SW. These factors limit the power of PM concentration alone to explain changes in

116   surface radiation.

117

118   Both field (Alton, North, & Los, 2007; Gu et al., 2002; Niyogi et al., 2004; Strada, Unger, & Yue, 2015)□

119   and modelling (Mercado et al., 2009; Rap et al., 2015; Roderick, Farquhar, Berry, & Noble, 2001; Xie et

120   al., 2020)□ studies have attempted to quantify the impacts of PM on vegetation, providing strong

121   evidence to support an increase in forest productivity, through increased surface diffuse light levels. A

122   smaller number of studies suggest a similar result for crops (Cheng et al., 2015; Gu et al., 2002; Li &

123   Yang, 2015)□. However, the magnitude of the benefit of increased proportions of diffuse light to

124   croplands is disputed. While some studies suggest increased diffuse fraction due to air pollution (Cheng

125   et al., 2015; Gu et al., 2002; Wang et al., 2015)□ increases gross primary production of crops, others

126   have found a reduction in predicted yields (Alton, 2008; Strada et al., 2015)□. Greenwald et al. (2006), for

127   example, predicted that crop yields may be reduced in a number of locations worldwide due to reductions

128   in total radiation offsetting gains in RUE from a higher diffuse fraction.

129

130   A range of factors may account for the varying results in the studies outlined above, and these merit

131   further investigation. One example is that the timing of changes in total SW and diffuse fraction relative to

132   crop development stage may impact yields. Crops progress through a series of characteristic

133   developmental stages; from sowing, to vegetative growth, to seed filling to harvest, with carbon allocated

134   in different proportions to different plant functions at each stage. Hence interventions to curb pollution,

135   including PM, may be more or less impactful at different times within the crop life cycle.

136

137   Here, the Joint UK Land Environment Simulator-crop (JULES-crop) model is used to explore the effect of

138   PM-mediated changes in light on maize yields across the NCP, and the sensitivity of the crops to the

139   timing of these changes. As discussed above, the interaction of PM with surface radiation is complex,

140   with concentration, composition and size distribution of the heterogenous mixture of PM particles all

141   contributing to the eventual impacts of PM on surface SW. We therefore study the effects of changes in

142   radiation directly, rather than considering fixed changes in PM concentration to determine how PM-

143   associated changes in total magnitude and temporal variability of SW (light intensity) and diffuse fraction

144   affect maize yields.

145

146 Novelly, we conduct a range of sensitivity tests to explore the response of simulated maize yield to

147 changes in total and diffuse SW, such as could result from policy interventions to reduce PM, at different

148 crop development stages. This facilitates understanding of how PM pollution affects yield differently when

149 it occurs at different development stages of our modelled crop. We then use time series of total SW and

150 diffuse fraction from other large global cities with differing PM pollution to investigate the impacts of

151 potential reductions in PM in the Beijing-Tianjin-Hebei region. Measurements of aerosol optical depth

152 (AOD) and total cloud cover are then used to demonstrate that changes in diffuse fraction and total SW

153 are linked to changes in PM. Furthermore, whilst previous authors (e.g. Greenwald et al., 2006)⬚ have

154 focused on cloud interactions with light, we use an average climatology to remove interannual variation in

155 cloud cover, allowing us to focus on the influence of PM under more stable cloud conditions. We achieve

156 this by manipulating SW and diffuse fraction, which we have shown to be strongly linked to aerosol optical

157 depth and therefore PM pollution in this region.

158

159 This paper therefore aims to explore how radiation profiles associed with levels of PM found in other city

160 regions may affect crop yields on the NCP, and to establish how targeted reductions in PM must take

161 account of the crop life cycle to achieve improvements in yield. Exploration of the developmental state

162 dependence of crop responses to PM linked radiation changes is key to ameliorating the impacts of PM

163 on crop production.

164

2. Materials and Methods

2.1 Model Set-Up

167 JULES-crop has been demonstrated to accurately simulate maize yields at several well-characterized

168 sites in the USA (Williams et al., 2017)⬚, although it has not previously been tested in the NCP. The

169 study domain (31.0 ˚N, 113.0 ˚E to 43.0 ˚N, 123.0 ˚E) spans a majority of the NCP including the Beijing-

170 Tianjin-Hebei region. The MODIS AQUA-TERRA land cover product MCD12C1 was used to determine

171 the cropped area of the NCP, which we assumed to be entirely given over to the major summer crop of

172 this region, maize. JULES-crop, within the Joint UK Land Environment Simulator (JULES) model version

173 5.3 was used to simulate yields across the cropped area (Best et al., 2011; Clark et al., 2011; Osborne et

174 al., 2015). We used the JULES-crop maize parameterization (Williams et al., 2017) with sowing dates

175 taken from Sacks et al. (2010). Crops were assumed to be well irrigated in all simulations. Following the

176 methodologies of Osborne et al. (2015),Williams et al. (2017) and Kimball et al. 2019, we convert the

177 carbon allocated to the harvestable portion of the simulated maize crop to yield (dry t ha^{-1}) .

178

179 Meteorological data of SW, downward long wave radiation, 2-m air temperature, precipitation, specific

180 humidity, surface pressure and wind speed were taken from ERA-5 (European Reanalysis 5th Generation)

181 for 1981-2017 at an hourly timestep and 0.25° spatial resolution (Copernicus Climate Change Service

182 (C3S), 2017). Diffuse radiation was calculated for each grid cell as the difference between the total and

183 the direct incoming SW radiation at the surface as given by ERA-5. Just over 45% the grid-cells in the

184 domain were assigned as maize using MODIS-terra land fraction products as given by ERA-5.

185

186 2.2 BASE Simulation

187 A climatological average driving dataset was obtained by calculating the mean of each meteorological

188 variable of the ERA-5 driving data at an hourly timestep for each grid cell for 1981-2017. This was used to

189 generate our baseline simulation (BASE) of maize production across the region. This average climatology

190 reduces interannual variability in SW and diffuse fraction, and allows us to focus on average variations in

191 SW and diffuse fraction and their relationship with one another. Perturbations are thereby compared to a

192 more stable average baseline. Linear and multi-linear regression were used to derive the relationships

193 between simulated yields and meteorological variables, and determine the relationships of diffuse fraction

194 and total SW radiation with one another and with simulated yield.

195

196 To assess whether increased diffuse fraction increases maize yield across the NCP independent of

197 changes in SW (as seen in previous studies; Rap et al., 2015; Roderick, Farquhar, Berry, & Noble,

198 2001b; Wickens & Horn, 1972), sensitivity tests were conducted in which the diffuse fraction was set to a

199 constant value throughout the year, ranging from 0 and 1, in increments of 0.1. The above sensitivity tests

200 and baseline results were used to generate relationships between total SW, diffuse fraction and maize

201 yield. These calculated relationships (Figure 1) greatly informed the experiments detailed below.

2.3 Driving Factors for Changes in SW and Diffuse Fraction

PM acts on incoming radiation in numerous and complex ways. Changes in concentration alone cannot be used as predictors of changes in radiation. Instead, the influence of PM speciation, size distribution, hygroscopicity and altitude, as well as meteorology must be considered both individually and in combination. Aerosol Optical Depth (AOD) on the other hand, has been demonstrated to be strongly linked to PM concentration (van Donkelaar, Martin, & Park, 2006)☐, whilst also incorporating the interaction of PM and meteorology, thus providing a better indicator of the net impact of PM on surface radiation where concentration alone may lead to erroneous conclusions (Qu, Wang, Zhang, Sheng, & Wang, 2016). AOD provides a measure of total column PM and its impact upon surface radiation (van Donkelaar *et al.*, 2013; Just *et al.*, 2015; Qu *et al.*, 2016; Qin *et al.*, 2018)☐. Least squares multilinear regression was applied (using the SKLearn python toolkit version 0.23.2) to AOD and total cloud cover (TCC), taken from the C3S meteorological datasets, to assess whether observed changes in SW and diffuse fraction on the NCP are driven by PM, cloud or both. The inclusion of TCC accounts for the impacts of PM on cloud formation, important given the contribution made by PM to cloud condensation, and thereby indirectly on incoming radiation. Our regression analysis was conducted using growing season average grid cell values of AOD, TCC, mean hourly daytime diffuse fraction for the growing season, mean hourly daytime downward SW radiation for the growing season, and final yield for the years 1997-2010.

2.4 Sensitivity at Different Development Stages

Varying meteorology and PM composition over the course of the year alter average total SW and diffuse fraction profiles across the NCP. The maize crop progresses through a series of development stages, characterised by different rates of photosynthesis and carbon allocation between roots, stems, leaves and reproductive structures. The impact of varying profiles of SW and diffuse fraction can therefore affect crop yields differently depending on when during the season perturbations to light occur. We conducted a range of sensitivity tests to assess how the timing of changes to the diffuse fraction and intensity of light relative to crop development stage affects final yield.

Post emergence, the crop develops through the vegetative stage and reproductive stage, each

230   subdivided into early and late in JULES, giving four stages overall. Increased levels of PM during each

231   development stage were simulated by elevating the diffuse fraction of our BASE simulation by 50% for a

232   given stage, and decreased levels of PM by reducing diffuse fraction by 50%. The relationship shown in

233   Figure 1. was then used to deduce the total SW for each timestep consistent with the altered diffuse

234   fraction. We refer to total SW modified in this manner as "diffuse-corrected" SW. All other driving variables

235   remain unchanged from BASE. The statistical significance of yield results were determined by related t-

236   test using the SciPy Stats module ttest_rel function across the cropped area of the model domain.

237 2.5 Impact of City Radiation Profiles on Yields

238   To investigate timing effects further, and as a proxy for potential future changes in PM concentration and

239   composition, we studied the impacts on NCP crop yields of light profiles from the regions surrounding four

240   global cities (New York, Madrid, Delhi, and Cairo), and one city in the NCP (Beijing).

241

242   These cities were chosen for their differing PM profiles and locations. Beijing experiences higher PM2.5

243   pollution (108 ± 34 µg m^{-3} for 2013-18, Zhai *et al.*, 2019) than Madrid (12.1 µg m^{-3} for the urban

244   background from 2004-2009, Karanasiou *et al.*, 2014) and New York (12.3 µg m^{-3} for the period 2005-

245   2016 (Peltier *et al.*, 2011)), but is located at a comparable latitude (Beijing: 39.9 ºN; New York: 40.7 ºN;

246   Madrid: 40.4 ºN). Conversely, Delhi experiences seasonally higher levels of PM pollution than Beijing

247   (varying from a minimum concentration of 46 µg m^{-3} to a maximum of 279 µg m^{-3} over the year; Gorai. A,

248   *et al.* 2018) but is located at a considerably lower latitude than Beijing. We therefore use Cairo (30.0 ºN)

249   as a comparator for Delhi (28.7 ºN) due to its similar latitude but lower PM pollution (51 µg m^{-3} in 2013,

250   Boman *et al.*, 2013), serving to illustrate how the meteorology and pollution profiles over Delhi city region

251   limit the potential surface SW in the region. Whilst the levels of PM in New York and Madrid are

252   substantially lower than those for Beijing and the NCP, large scale PM reductions across the NCP are

253   likely and possible given the trajectory of PM concentrations over the last 7 years. We therefore present

254   this city analysis as a way to explore how SW and diffuse fraction and therefore crop yields could change

255   in the near future. They should be seen as an exploration of possibility space in terms of the outcomes of

256   PM linked changes to SW and diffuse fraction, not an explicit prediction for what the future will definitively

257   look like.

258

259   Average hourly diffuse fractions (taken from the 37-year ERA-5 dataset) from each city, were used to

260   drive JULES-Crop over the model domain. The resulting yields on the model domain using SW and

261   diffuse fraction profiles from four global city regions were compared to those obtained using the diffuse

262   fraction for Beijing, and to our climatological average BASE case. The climatological average total SW for

263   each city region was then applied in conjunction with the climatological average diffuse fraction time

264   series to simulate the net effects of these different city PM regimes on NCP maize yields.

265

266   To disentangle the opposing effects of changes in SW and diffuse fraction on yield, we ran two further

267   simulations for each city to demonstrate: 1) the levels of SW that would be found to occur in each city

268   given the diffuse fraction at that time in the NCP, 2) the potential impacts of an altered relationship

269   between SW and diffuse fraction, which can be partially attributed to changing levels of PM. In the first

270   simulation, the mean diffuse fractions for the NCP domain were applied to each grid cell (as per BASE),

271   with the total SW for that grid cell, derived from the relationship between diffuse and total SW for that city

272   (named CITY_mod_SW simulations). In the second simulation, mean total SW for the NCP domain was

273   applied to each grid cell (as per BASE), and the diffuse fraction for that grid cell was derived from the

274   relationship between diffuse and total SW for that city (CITY_mod_Diff simulations). These simulations

275   superimpose the relationship between SW and diffuse fraction in other city regions over the NCP. As this

276   relationship between total and diffuse SW is strongly linked to levels of cloud and aerosol, if can be

277   considered a proxy to describe the effects of changing profiles of SW and diffuse fraction over the year on

278   the NCP.

279   3. Results

280   3.1 Aerosol Optical Depth (AOD) Results

281   We found the strongest correlation between changes in AOD and total cloud cover (TCC) with diffuse

282   fraction (R^2=0.90), whilst changes in AOD and TCC explained just under 40% of variation in total SW.

283   AOD alone was found to explain 80% of changes in diffuse fraction but only 15% of changes in total SW.

284   This suggests that of the variability in SW resulting from changes to cloud and aerosol, an average of

285   38% comes from aerosol alone (R^2 for aerosol alone divided by R^2 for aerosol + total cloud cover). We

286   conclude that whilst the observed changes in light intensity in the domain are mainly driven by cloud

287   cover, changes to AOD, linked to PM pollution, make a non-negligible contribution to light intensity, and a

288   large contribution to changes in diffuse fraction. Further sensitivity tests presented here, in which we

289   modify light intensity (SW) and/or diffuse fraction, should therefore be seen as an exploration of potential

290   changes in maize yields if PM concentrations were to change across the NCP.

3.2 The BASE Simulation

3.2.1 Relationships

293   We found light to be the most critical meteorological variable for predicting simulated maize yield in our

294   baseline simulation (BASE). Yield was positively correlated with mean hourly SW such that a 10%

295   increase in light intensity correlated with an 8% increase in yield (R^2=0.54, Figure 1.i). However, we found

296   yield to be negatively correlated with mean hourly diffuse fraction with a 10% increase in diffuse light

297   reducing yield by 9% (R^2=0.49, Figure 1.ii). While this may initially appear counterintuitive, it is driven by

298   the strong negative logarithmic relationship between grid cell average total SW and diffuse fraction

299   (R^2=0.85) for the domain during the growing season (Figure 1.iii.), therefore reproducing the negative

300   impacts of reduced SW from increased PM cover reported in previous studies (Gu, Wang, Zhuang, &

301   Han, 2018; Zhou, Chen, & Tian, 2018). A 10% increase in the mean growing season diffuse fraction (i.e.

302   from 0.49 to 0.54) on the NCP corresponds to a reduction in average SW of 72 W m^{-2}.
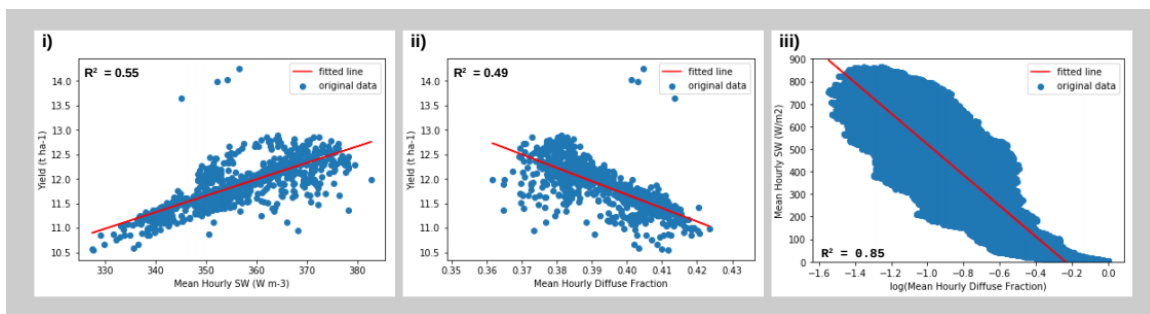
303

304   Figure 1) i) Maize yield versus BASE average hourly SW in grid cells with saturated soil, ii) BASE average hourly diffuse fraction vs

305   yield in saturated soil grid cells iii) BASE SW vs diffuse fraction for all grid-cells.

306   The relationship between diffuse fraction and yield was non-linear for constant total SW. Increasing

307   diffuse fraction by 10% relative to the growing season mean increased simulated maize yield by 0.007 t

308   ha^{-1}, while a 10% decrease reduced yield by 0.035 t ha^{-1}.These changes, associated with changing

309   diffuse fraction, represent less than a 0.1% change in yield, whereas a 10% increase in average total SW

310   led to a yield gain of 1.05 t ha^{-1}, a change 150 times greater. We conclude therefore that the diffuse light

311   fertilisation effect is insignificant in comparison to the effects of reducing total SW.

312 3.2.2 Yields

313   The average yield predicted across the NCP was 11.9 ± 0.5 t ha^{-1} , using the 37-year climatological

314   average driving data derived from ERA-5. In 2011, the recorded yield for maize in China was 5.75 t ha^{-1}

315   (Hu and Zimmer, 2013), just under half the modelled yield produced in our BASE simulation. Without

316   irrigation however, the modelled average yield is 6.73 t ha^{-1}. Furthermore, we made the assumption that

317   maize is grown across all cropped land in the model domain, whereas in reality the most favourable areas

318   for crop production are currently reserved for other crops. This results in a further positive skew of

319   average maize yield in our simulations.

320

321   To ensure that light effects are not confounded with other environmental limitations, we continue to apply

322   irrigation in all simulations comparing results against the (irrigated) BASE simulation. The projected yields

323   for all model simulations are shown in Table 1. The cropped area and yields for BASE, along with the

324   average SW and diffuse fraction across the domain, are shown in Figure 2. Table 1 provides a reference

325   for the wide range of potential yields that might be expected under the SW and diffuse fraction scenarios

326   explored in this work.

327
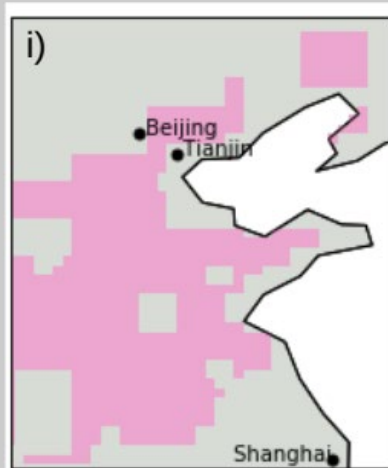
i) Cropped Area
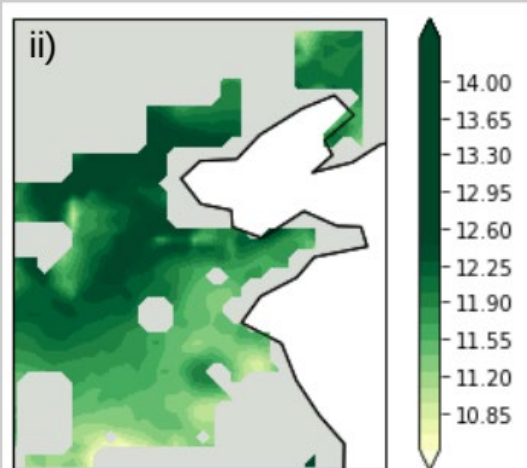
ii) Maize Yield (t ha⁻¹)
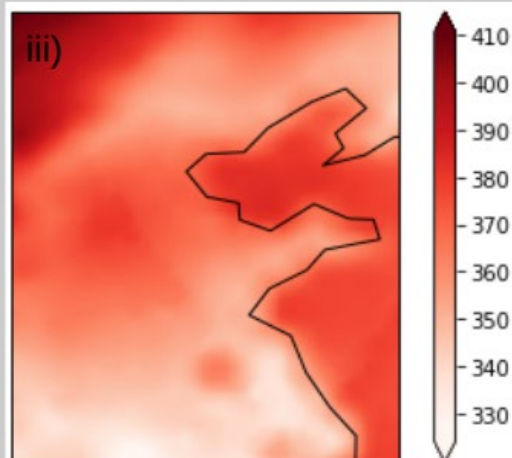
iii) Average Growing Season Hourly SW (W m⁻¹)
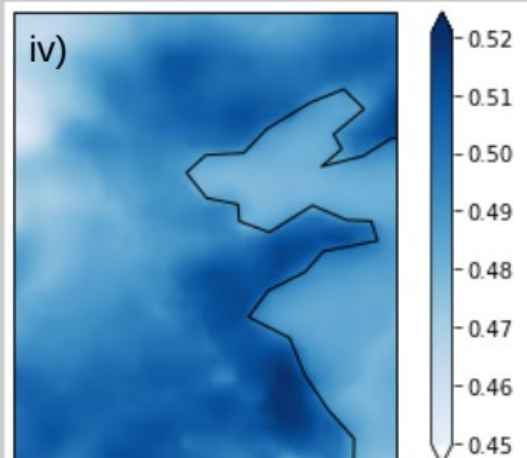
iv) Average Growing Season Hourly Diffuse Fraction

329   Figure 2) i) Cropped region of the NCP in model, ii) BASE model yield output (t ha^{-1}), iii) Average Growing Season Day time Hourly

330   SW (W m^{-3}), iv) Average Growing Season Day Time Hourly Diffuse Fraction

331

332   Spatial variation in maize yield across the NCP in BASE was highly related to the strong negative

333   logarithmic relationship between SW and diffuse fraction. In the BASE_Diff simulations, where diffuse

334   fraction was increased without a change in total SW, maize yield slightly increased due to the diffuse light

335   fertilisation effect, as reported for a variety of crops in previous modelling and observational studies

336   (Mercado *et al.*, 2009; Brodersen and Vogelmann, 2010; K. Huang *et al.*, 2014; Rap *et al.*, 2015, 2018;

337   Yue and Unger, 2017)◻. However, as shown in Figure 1, this relationship is not observed for our BASE

338   case (Figure 1.i.). This is due to the observed reduction of SW with increasing diffuse fraction In Figure

339   1.iii.

340

Run #	Name	Average Yield ± Standard Deviation (t ha^{-1})	Percentage Difference from BASE (%)
1	BASE	11.9 ± 0.5	N/A
2	BASE_Diff_0.0	10.2 ± 0.5	-14.1
3	BASE_Diff_0.1	10.7 ± 0.5	-9.8
4	BASE_Diff_0.2	11.2 ± 0.5	-5.9
5	BASE_Diff_0.3	11.6 ± 0.5	-2.4
6	BASE_Diff_0.4	11.9 ± 0.5	0.6
7	BASE_Diff_0.5	12.3 ± 0.5	3.1
8	BASE_Diff_0.6	12.4 ± 0.5	5.3
9	BASE_Diff_0.7	12.8 ± 0.5	7.0
10	BASE_Diff_0.8	12.8 ± 0.5	8.4
11	BASE_Diff_0.9	12.3 ± 0.5	9.5
12	BASE_Diff_1.0	12.9 ± 0.5	10.1
13	BJG, Diff	11.9 ± 0.5	1.1
14	MAD, Diff	11.4 ± 0.5	-34.2
15	NYC, Diff	11.7 ± 0.5	7.1
16	DEL, Diff	11.7 ± 0.5	-17.6
17	CAI, Diff	11.2 ± 0.5	-31.7
18	BJG_SW, Diff	12.1 ± 0.4	2.5
19	MAD_SW, Diff	15.2 ± 1.2	28.9
20	NYC_SW, Diff	12.6 ± 0.4	5.7
21	DEL_SW, Diff	11.9 ± 0.5	-0.1
22	CAI_SW, Diff	15.9 ± 2.1	34.2
23	BJG_Mod_Diff	11.7 ± 0.5	-1.1
24	MAD_Mod_Diff	11.6 ± 0.5	-3.0
25	NYC_Mod_Diff	11.7 ± 0.5	-1.7
26	DEL_Mod_Diff	11.6 ± 0.5	-3.2
27	CAI_Mod_Diff	11.6 ± 0.5	-3.2
28	BJG_Mod_SW	11.9 ± 0.7	1.1
29	MAD_Mod_SW	7.9 ± 0.7	-34.2
30	NYC_Mod_SW	12.6 ± 0.5	7.1
31	DEL_Mod_SW	9.8 ± 0.7	-17.6
32	CAI_Mod_SW	8.1 ± 0.5	-31.7
33	DEV1_0.5	13.3 ± 0.9	6.6
34	DEV2_0.5	13.5 ± 1.4	8.3
35	DEV3_0.5	15.9 ± 1.4	28.2
36	DEV4_0.5	15.1 ± 1.2	21.6
37	DEV1_1.5	8.4 ± 1.2	-33.1
38	DEV2_1.5	8.2 ± 1.1	-33.5
39	DEV3_1.5	7.9 ± 0.7	-37.3
40	DEV4_1.5	9.5 ± 0.9	-24.4

341

342 **Table 1.** Summary of key model results from simulations. Average yield is colour coded such that the average yield for BASE is the

343 midpoint, with 0% change as the mid-point, red for decreasing yield, and blue for increasing. The percentage difference from base is

344 colour coded 0% difference from BASE as white and the largest difference as the most purple.

345

346 Key:

347 BASE simulations provide a climatological average for comparison of sensitivity tests to a reasonable baseline scenario.

348

349 BASE - a simulation using the climatological average meteorological driving data

350

351 BASE_Diff_x – Uses climatological average meteorological driving data, excepting diffuse fraction, which was set to a fixed fraction

352 (x). This baseline scenario provides a benchmark to demonstrate the effects of diffuse fraction modification alone.

353

354 BJG , MAD, New York, DEL, CAI – Beijing, Madrid, New York City, Delhi, Cairo

355

356 CITY simulations are used to illustrate potential future scenarios for yield on the NCP with changing SW radiation profiles.

357

358 CITY, Diff – As BASE, but with diffuse fraction from CITY across all grid cells for each timestep.

359

360 CITY_SW, Diff – As BASE, but with SW and diffuse fraction from CITY across all grid cells for each timestep

361

362 CITY_Mod simulations are used to present the relationship between diffuse fraction and SW found at CITY in the context of the

363 NCP as a proxy for the differing conditions and PM profiles found at each CITY region.

364

365 CITY_Mod_Diff - As BASE, but with diffuse fraction derived from NCP SW using the relationship between SW and diffuse fraction

366 found at the CITY.

367

368 CITY_Mod_SW – As BASE, but with SW derived from NCP diffuse fraction using the relationship between SW and diffuse fraction

369 found at the CITY.

370

371 DEV simulations test crop sensitivity to changes in SW and diffuse fraction during different crop development stages.

372

373 DEV1 , DEV2, DEV3, DEV4 – Early vegetative phase, late vegetative phase, early reproductive phase, late reproductive phase

374

375 DEVZ_0.5 – As BASE, but with diffuse fraction decreased by 50% for development stage Z, with SW set to "diffuse corrected" SW.

376

377 DEVZ_1.5 – As BASE, but with diffuse fraction increased by 50% for development stage Z, with SW set to "diffuse corrected" SW.

378 ## 3.3 Sensitivity at Different Development Stages

379 The timing of the changes in SW and diffuse fraction made significant differences to final maize yield. We

380 found maize to be most sensitive to changes in SW intensity and diffuse fraction during the early

381 reproductive stage (DEV3). Increased diffuse fraction and reduced SW (representative of an increase in

382 PM concentrations) during this period have the most significant effect, reducing yields by an average 37%

383 compared to BASE (Paired t-test, t=-5.73, p=0.001). Conversely, reducing diffuse fraction and increasing

384 SW (simulating reduced PM) during DEV3 led to a 28% increase in average yield (Paired t-test, t=-6.46,

385 p=0.001). Applying the same changes to light intensity (total SW) and diffuse fraction during other

386 development stages had a lower impact. For example, simulating reduced PM during the early vegetative

387 stage (DEV1) increased yields by only 7%, less than one-fifth of the impact for DEV3 (again, the

388 difference here is significant, t=-5.78, p=0.001). However, the difference between yields when diffuse

389 fraction is reduced in the early and late reproductive phase was not found to be significant (t=-2.49,

390 p=0.139), and neither was the difference between increasing diffuse fraction in the vegetative or early

391 reproductive phase. This indicates that changes in radiation during the early reproductive phase produce

392 the most sizable increases in maize yields, but that increasing ambient SW radiation by reducing the level

393 of PM during the late reproductive phase would also be beneficial.

394 ## 3.4 Impact of City Radiation Profiles on Yields

395 The global city regions used to simulate crop yields if PM was to change across the NCP, are

396 summarised in Table 2 below.

397

398

399

Location	Coordinates	Average Hourly SW (W m-2)	Average Hourly Diffuse Fraction	Average AOD	PM2.5 (µg m-3)
NCP	31.0N, 113.0E to 43.0N to 123E	363.5	0.49	0.37	62.5-92.7
Beijing	39.9 °N, 116.4 °E	365.6	0.51	0.28	108.0
Madrid	40.4 °N, 3.7 °W	453.2	0.37	0.15	12.1
NYC	40.7 °N, 74 °W	377.6	0.42	0.20	12.3
Delhi	28.7 °N, 77.1 °E	408.5	0.44	0.38	46.0-279.0
Cairo	30.0 °N, 31.2 °E	547.8	0.33	0.17	51.0

400   Table 2. Indicative values for average SW, diffuse fraction and PM2.5 concentration for NCP study region and for city regions

401   studied.

402   Average hourly SW and diffuse fraction are taken from the climatology (generated from 1979-2017 ERA-5 meteorological data) used

403   to drive all city runs for the growing season of modelled maize crop.

404

405   AOD is an average value, taken from the C3S climate data store meteorological dataset for aerosol optical depth, for the city

406   containing grid cell, for the months April to September (inclusive of growing season), from 1997-2010

407   PM2.5 data is taken from a range of ground-based studies conducted during the timeframe of this modelling study. Though the PM

408   concentrations are not always overlapping in time in many cases, this serves as an indicator of representative values within the

409   period of the climatology.

410   a). Yao. L, et al., 2016 (range given for average seasonal values) b). Zhai. S, et al., 2019, c). Santurtun, A, et al., 2015, d). Shmoo,

411   J.L.C., et al., 2016, e). Jain, S.L., et al., 2005, (range given for average seasonal values) f). Khoder, M.I., et al., 2009

412

413   When values of SW and diffuse fraction taken from Beijing city were applied across the domain, yields

414   did not differ significantly from those obtained using SW and diffuse fraction for the whole of the NCP

415   domain. All other city comparison runs discussed in this section are compared to yields from Beijing

416   (BJG) simulations rather than BASE, because the different spatial distribution of SW and diffuse fraction

417   in BASE would make such comparison inappropriate.

418

419   The greatest change from our Beijing-based simulations was found in applying values for Cairo to the

420   NCP. CAI_Diff (i.e. NCP domain SW but Cairo diffuse fraction) simulated yields 34% lower than those of

421   BJG_Diff (Figure 3.e.i), mostly attributable to average diffuse fraction in Cairo being 35% lower than that

422   in Beijing during the growing season. Application of diffuse fractions from New York, Madrid and Delhi to

423   the NCP (New York_Diff, MAD_Diff, DEL_Diff simulations) reduced yields by an average of 1, 5 and 1%

424   respectively due to slightly lower annual average diffuse fractions (0.42, 0.37 and 0.44, respectively)

425   reducing diffuse light fertilisation effects.

426

427   However, when both diffuse and total SW were modified to reflect the average conditions in each city, the

428   higher average annual SW at New York, Madrid and Cairo more than compensates for their relatively

429   lower diffuse fraction, with yields increases in New York_SW_Diff, MAD_SW_Diff and CAI_SW_Diff

430   simulations by 3%, 26% and 30% respectively (Figure 3.c,e,ii). Although SW and diffuse fraction are

431   substantially different at Delhi from Beijing, DEL_Diff and DEL_SW_Diff (described in section 2.5) show

432   little change in yield from BJG_Diff (-1%) and BJG_SW_Diff (-3%) respectively.
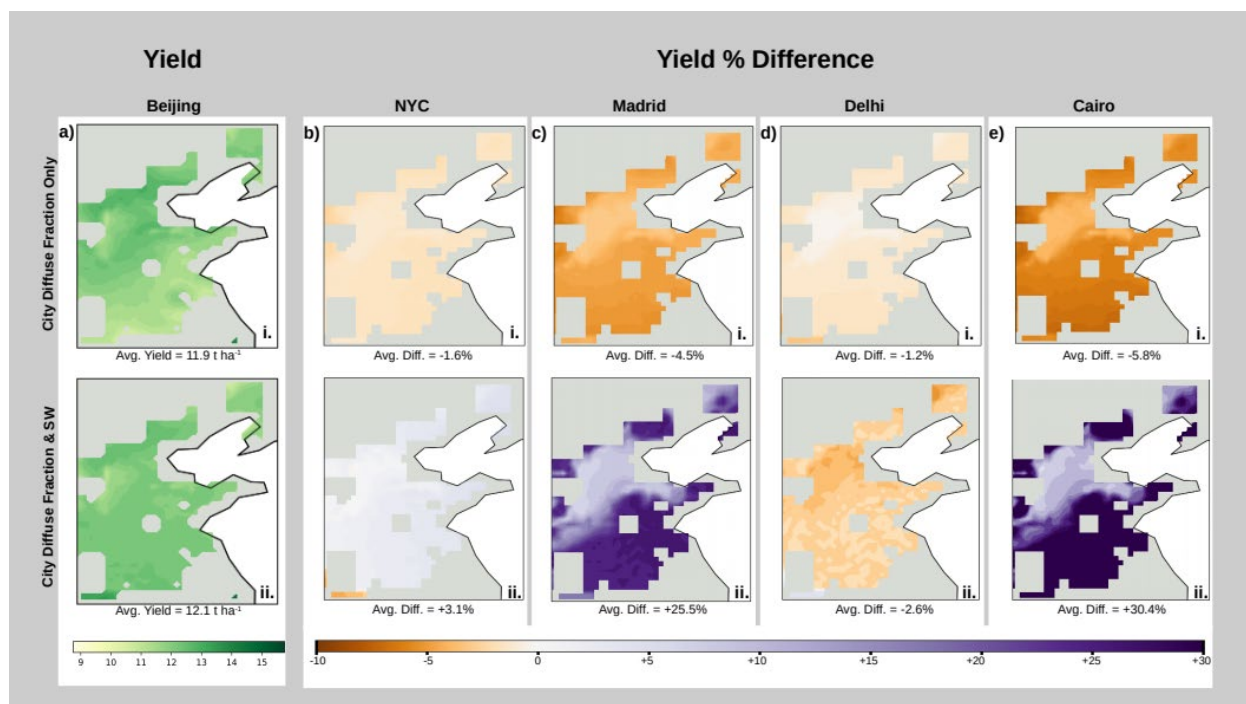
433   Figure 3) a) Yields (t ha⁻¹) for city radiation profile simulations i. BJG_Diff and ii. BJG_SW_Diff. Fig1.b-e) percentage difference

434   between i. <CITY>_Diff and BJG_Diff, and ii. <CITY_ SW_Diff and BJG_SW_Diff, for b) New York, c) Madrid, d) Delhi and e) Cairo.

435

436   Simulations using city-modified diffuse fractions (i.e. those generated using the relationship between total

437   SW and diffuse fraction at each city, Figure 4.c-f.i.) showed a negligible reduction in yield compared to

438   BJG_mod_Diff (Figure 4.c-f.ii.). Furthermore, yields simulated using SW derived from the relationships for

439   Madrid, Cairo and Delhi (Figure 4.d-f.ii), are lower than those for BJG_mod_SW, with reductions of 35, 32

440   and 18% respectively. This can be explained in each case by lower total SW in that location for the

441   diffuse fractions found on the NCP. In contrast to the other city regions, modified SW from New York

442   increased yields by an average of 5.9% (Figure 4.c.ii). as SW in New York is higher for a given diffuse
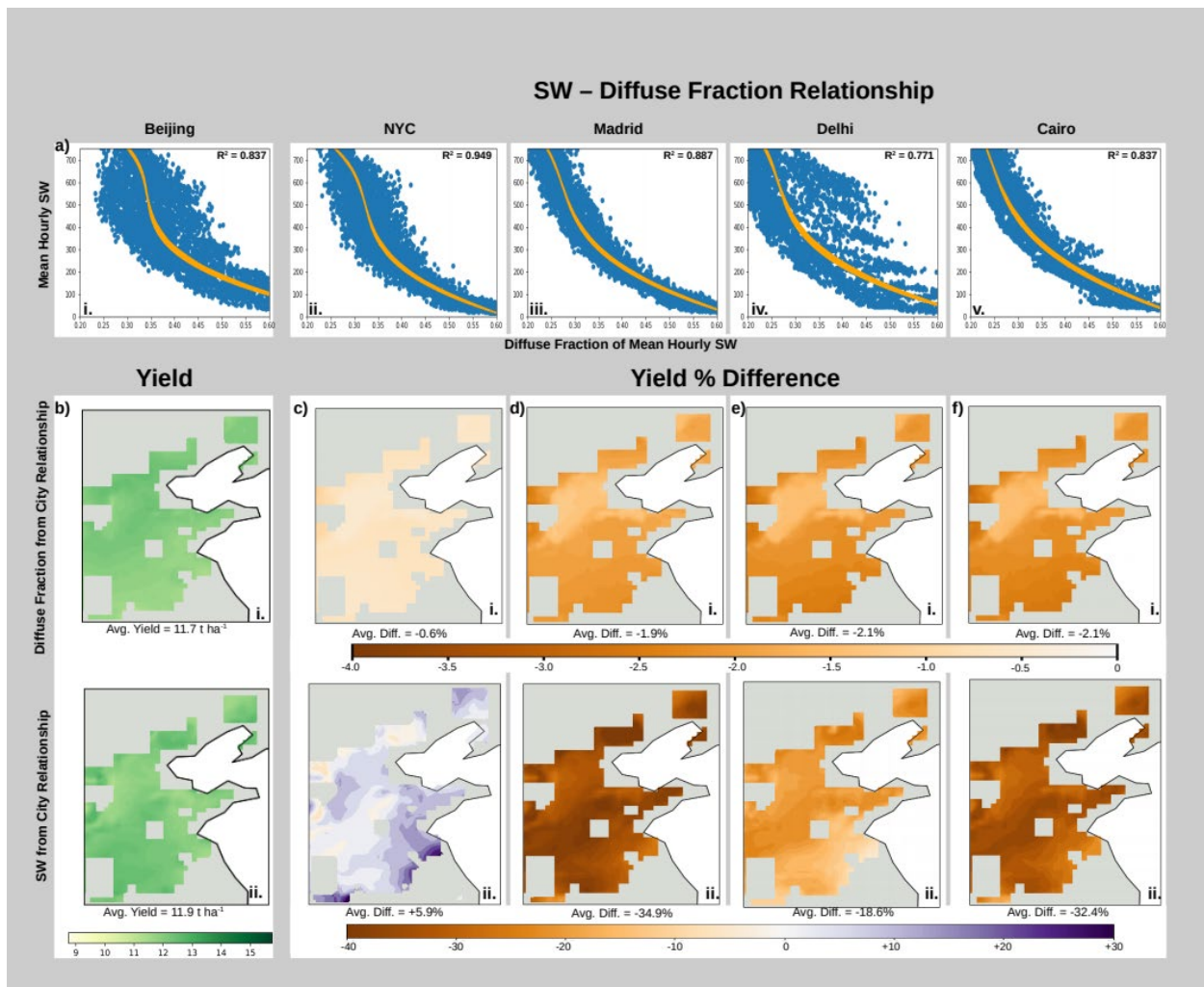
443   fraction in the NCP.

Figure 4.a.i-v) Relationships between SW and Diffuse fraction for each city, with data points in blue and quadratic regression line in orange.

Figure 4) b) Yields for CITY_MOD radiation profile simulation. BJG_Mod_SW and ii. BJG_Mod_Diff

Figure 4.c-f) percentage difference between i. <CITY>_Mod_Diff and BJG-Mod_Diff and ii.<CITY>_Mod_SW and BJG_Mod_SW, for c) New York, d) Madrid, e) Delhi and f) Cairo.

4. Discussion

4.1 PM influences Maize Yields

The timing of changes in radiation relative to the developmental stage has the greatest impact during the early reproductive phase. This result has key implications for the nature and timing of emission reductions which may have greatest impact for yield crop yields on the NCP. In line with field observations, the photosynthetic capacity and hence carbon assimilation rate of maize in JULES-crop increases with leaf area during the vegetative development stage, peaking during the late vegetative stage , and remaining

20

456 high during the early reproductive stage. However, at the start of the early reproductive phase, the maize

457 plant has matured, and therefore carbon allocation is diverted from stem, leaf and root to the harvestable

458 portion. Our analyses demonstrate that the maize crop is most sensitive to reductions in SW (linked to

459 elevated diffuse fraction) during the early reproductive phase (DEV3_1.5) (see Table 1). Similarly, the

460 greatest predicted increase in yield results from reductions in diffuse fraction (i.e. reduced PM) in the early

461 reproductive phase (simulation DEV3_0.5, Table 1), which occurs during July in our modelled maize

462 season. As discussed earlier, at this time of year, PM concentration is at a minimum but AOD reaches a

463 maximum in the NCP due to prevailing meteorology interacting with PM pollution to produce haze (Qu *et*

464 *al.*, 2016). Whilst this indicates a smaller contribution from AOD to SW variability during this period, our

465 analyses demonstrated that aerosol still contributes 32% of the total variability in SW during the early

466 reproductive phase, i.e. PM still exerts an important influence on SW during this period. The remaining

467 variation not due to cloud and aerosol simply originates from variations in latitude and altitude across the

468 NCP, alongside seasonal variation in incoming radiation. The relatively small change in the AOD – SW

469 relationship between seasons despite large changes in PM concentration and composition highlights the

470 importance of using AOD as a measure of the impact of PM, rather than simply using PM concentration.

471 The complex interplay of PM and meteorology, alongside factors such as PM speciation and size

472 distribution, it impossible to predict how increases or decreases in bulk PM concentration will affect crop

473 yield. PM pollution at a given time of year can thus have a disproportionate impact relative to its

474 concentration. To increase crop yields, then, policymakers should make targeted emission reductions

475 during the early reproductive phase of regional crops when reduced PM concentrations may be expected

476 to have a far greater impact on yields than at other times of year.

477

478 PM concentration in the NCP fell by ~30% between 2013 and 2017 (Zhai *et al.*, 2019) following the

479 Chinese Government's introduction of the "Action Plan on the Prevention and Control of Air Pollution" in

480 2013. Despite these reductions, annual average PM2.5 concentrations for the Beijing-Tianjin-Hebei

481 region were still well above national and international annual mean guidelines of 35 µg m^{-3} and 10 µg m^{-3}

482 respectively (China: Air Quality Standards | Transport Policy, 2013; WHO, 2015), whilst recurrent haze

483 events remain a pressing issue limiting visibility and reducing total SW at the surface (Guo *et al.*, 2014;

484 An *et al.*, 2019; Zeng *et al.*, 2019). Although PM pollution is decreasing on the NCP, our simulations

485 suggest that the relatively high PM concentrations still present will continue to limit potential maize yield.

486 Several factors contribute to the impact of PM on crops, and these are discussed below.

487

4.2 Radiation from Comparable Cities alters Maize Yields

489 Average maize yield increased by as much as 29% (Figure 3b-c, e.ii., Table 1) when the climatological

490 average total SW and diffuse fraction at Madrid, New York or Cairo, which have lower average PM

491 concentrations than Beijing, are applied across the NCP. Conversely, when light conditions from Delhi are

492 applied, average maize yields remain virtually unchanged. We ascribe these effects to the combination of

493 the magnitude and seasonality of changes in SW and diffuse fraction at each city (see Figure 5 below).
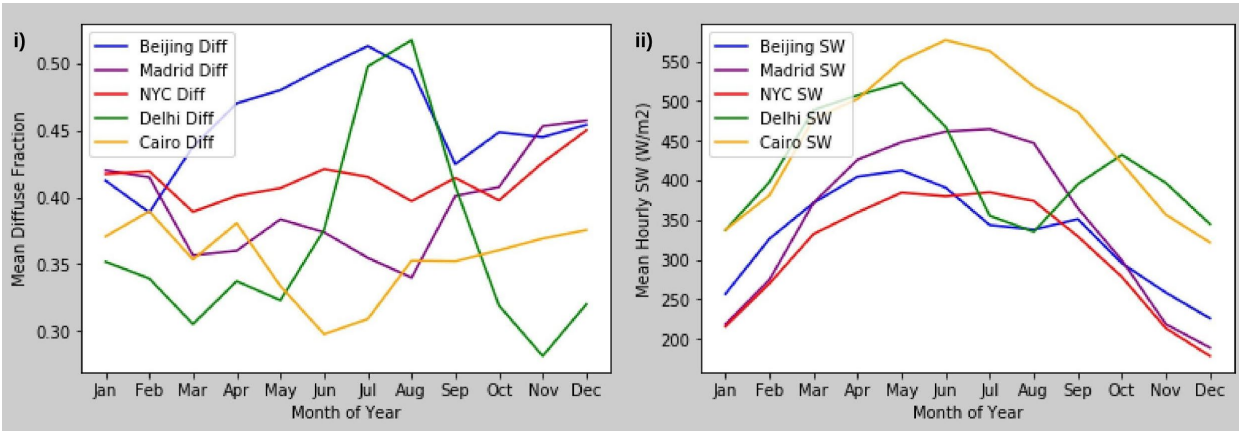
494

495

496 Figure 5. i) Average monthly diffuse fraction for Beijing, Madrid, New York, Delhi and Cairo. ii) Average

497 hourly downward SW radiation per month for Beijing, Madrid, New York, Delhi and Cairo.

498

499 Heavy cloud cover associated with the Indian monsoon reduces total SW in Delhi in July and August

500 (Figure 5.i.). Although partially compensated by a large increase in diffuse fraction, the net effect is still a

501 reduction in maize yields across the NCP. The higher SW and lower diffuse fraction seen during the rest

502 of the year do not fully compensate the changes in light profile during this critical period. Whilst the

503 changes at Delhi are driven by seasonal increases in cloud cover, modelling studies suggest that despite

504 the increase in wet deposition from increased rainfall in this time period, anthropogenic and natural

505 aerosol do contribute to the reduction in total SW (Kuhlmann and Quaas, 2010). This reduction during the

506 period corresponding to the early and late reproductive phase has greater impact on maize yield than the

507 higher SW during the rest of the growing season, in line with the results from our development stage

508 simulations. Results presented in the wider literature suggest that reductions in light intensity on the NCP

509 during late summer may result from PM-linked haze events (Chameides *et al.*, 1999; Zhou *et al.*, 2019)□.

510 Reducing aerosol pollution at this time of year would therefore increase light intensity for crop

511 photosynthesis. Interventions during less developmentally critical stages may have smaller effects than a

512 similar magnitude of intervention carried out during the early crop reproductive stage.

513 4.3 How PM might change Radiation in the Future

514 Despite similar annual mean PM concentrations in Madrid and New York (Karanasiou *et al.*, 2014; Peltier

515 *et al.*, 2011), there are large differences in yield between simulations driven with SW and diffuse fraction

516 from Madrid (MAD_Diff_SW) and New York (New York_Diff_SW). This yield gap is the result of ~20%

517 higher mean SW in Madrid than New York during the growing season (Figure 5) which is driven by

518 differences in meteorology, including cloud cover, between the two locations. The meteorology of the

519 NCP encourages formation of fog as well as haze, driven by the high relative humidity (Quan *et al.*, 2011;

520 Gao *et al.*, 2015; Yang *et al.*, 2020). Given the higher average ambient SW at Madrid than in the NCP

521 throughout the entire year, it is likely that yield increase is not solely attributable to PM, and that reduced

522 NCP PM concentrations would result in more modest yield gains than those seen in MAD_SW_Diff. Given

523 New York's more comparable SW profile during the growing season, excepting the critical months of July

524 and August, application of New York SW and diffuse fraction (New York_SW_Diff) may provide a more

525 realistic future scenario for the NCP if July and August AOD could be reduced through reductions in PM

526 concentrations. Though such increases would be relatively small, as differences in daylength and cloud

527 cover have more substantive effects, the 3% rise in yields seen for New York_SW_Diff would equate to a

528 gain of approximately 8 Mt of maize nationwide, sufficient to offset the maize annually imported by China

529 (FAOSTAT 2020), so increasing both national and global food security while increasing economic well-

530 being of NCP farmers.

531

532 Contrastingly, if PM pollution intensifies across the NCP during the late vegetative or early reproductive

533 phase, yields may further decline. As seen from simulations using Delhi SW and diffuse fraction, the drop

534 in light intensity during July and August reduces yields, despite a ~12% higher average growing season

535 SW in Delhi than Beijing. Although Delhi's annual decrease in light intensity during DEV3 is mainly

536 attributed to cloud cover, two key lessons can be learnt from the case of Delhi. Firstly, if reductions in SW

537   radiation, similar in magnitude to the seasonal reduction in SW seen in Delhi, were to occur in the NCP, it

538   would be detrimental to crop yields in the region. Secondly, although reductions in SW radiation have

539   most impact during DEV3, they also reduce plant growth at other development stages, as found in

540   simulations DEV1_1.5 and DEV2_1.5. It is likely that increasing PM concentrations in Delhi and its

541   surrounding regions have reduced crop yields in the Indo-Gangetic Plains in recent years (Burney and

542   Ramanathan, 2014; Mina *et al.*, 2018b). Any reversion to higher PM emissions on the NCP would likely

543   have a similar effect.

544

545   Furthermore, the Delhi and New York simulations demonstrate that reductions in PM during the

546   vegetative or late reproductive phases would likely have little impact on yields overall. Increased SW in

547   Delhi, and decreased SW in New York during these time periods does not outweigh the impact of

548   changes in SW during the early reproductive phase. The particular timing of changes in PM then, is

549   especially impactful. Increased total SW during the crop vegetative stage or the late reproductive stage

550   would not be sufficient to significantly increase yields if PM pollution remained high during the early

551   reproductive phase. Similarly, we see in New York that elevated SW during the early reproductive phase

552   may be sufficient to compensate, or even increase, yields if PM remained high at other times of year.

553   4.4 Comparison to previous studies

554   Our results highlight the key role of the timing of changes to PM pollution relative to crop development

555   stage, while adding further evidence to a growing body of research describing the net negative impact of

556   PM pollution upon crop yields. Whilst a number of modelling studies suggest there exists an optimum

557   diffuse fraction for growth and yield, we do not see this for the range of diffuse fractions realistic of those

558   observed across the NCP. We attribute this to the strength of the non-linear negative relationship

559   between diffuse fraction and total SW, and further link this to changes in AOD and PM.

560

561   The timing of changes in PM concentration, size distribution and composition is an understudied aspect of

562   PM impacts on crop yield. We find that the effect from increased SW is greatest during the early

563   reproductive stage, when crops allocate carbon to seed. Our analysis of light profiles from a range of city

564   regions further emphasises the time dependency of PM impacts. This novel analysis stresses the need

565   for targeted intervention by policy makers trying to achieve higher yields by reducing PM, and highlights

566 the necessity of further field studies to characterise PM burden at times of year corresponding with the

567 early reproductive stage for crops in different world regions.

568

569 4.5 Uncertainties and Future of Maize Yields on the NCP

570 Factors other than light intensity and the ratio of diffuse to direct light influence crop production. To

571 remove water stress, a key environmental stressor, as a confounding factor we assumed the region

572 irrigated as reported to be the predominant practice (Yang et al. 2015). This assumption enables us to

573 study light effects in isolation. Additional validation of modelled yields against reported harvests for the

574 NCP would enable maize in JULES-Crop to be parameterised for region-specific maize varieties and

575 agronomic practice, e.g. irrigation regimes and crop losses during harvesting, increasing confidence in

576 our model projections of actual yield. Whilst JULES-crop includes a general parameterisation for crop

577 response to changes in the diffuse fraction of SW radiation, future research is required to establish the

578 specific response of a maize canopy. However, given the dominance of the impact of changes in SW on

579 crop yields over changes in diffuse fraction seen here, we would expect only minor changes in projected

580 crop loss as a result.

581

582 Similarly, our analysis relies upon the strength of the reanalysis data provided by ERA-5. Whilst a

583 significant proportion of these data are model- rather than observation- derived, this dataset represents a

584 significant step forward from similar reanalysis datasets (Copernicus Climate Change Service (C3S),

585 2017; Urraca et al., 2018)□, and provides radiation data comparable to satellite retrievals. A recent review

586 identifies an underestimate of diffuse light by ERA-5 compared to some satellite retrievals (Jiang, Yang,

587 Wang, Bai, & Bai, 2020)□ but the sparse ground measurement sites used within that study demonstrate

588 the need for large-scale reanalysis data to be used for modelling studies addressing a large geographical

589 region. Only two ground stations used by these authors lie within our model domain. Given our use of

590 climatologically averaged data to drive our model, we feel confident that the ERA-5 dataset represents

591 the most useful assessment of surface radiation for our purposes and is suitable for use over the

592 geographical and temporal scales of our simulations.

593

594 A positive contribution from diffuse radiation to plant photosynthesis rates has been well documented for

595 tree species (Roderick *et al.*, 2001; Niyogi *et al.*, 2004; Mercado *et al.*, 2009; Kanniah *et al.*, 2012; Rap *et*

596 *al.*, 2015), but the net impact on crop yields of increased diffuse fraction at the expense of light intensity is

597 less well understood. We find that the decrease in total SW associated with increasing PM concentrations

598 far outweighs any possible fertilisation effect of increased diffuse fraction. Breeding programmes have

599 already delivered substantial increases in leaf angles in the upper canopy of maize, increasing light

600 penetration to the lower canopy such that maize might be expected to benefit less from diffuse light

601 fertilisation than tree species (Hammer et al. 2009; Zhu et al. 2010). We find that the decrease in total SW

602 associated with increasing PM concentrations far outweighs any possible fertilisation effect of increased

603 diffuse fraction. Elevated PM during the early reproductive stage (i.e. flowering and pod filling) would be

604 particularly detrimental to crop development, with a 50% increase in diffuse fraction during this period

605 reducing yield by an average of 37% due to the accompanying reduction in SW. Although cloud cover

606 plays a greater role in the attenuation of SW radiation than PM, our analysis of AOD and total cloud cover

607 demonstrates that aerosol contributes a third of the observed change in SW. Our sensitivity analyses

608 based on light intensity and diffuse fraction over New York suggests that an increase in maize yields of up

609 to 3.5% may be realistic for NCP if PM concentrations were to be reduced to those of New York. This will,

610 however, depend on the concomitant changes in particle size and composition, which further affect the

611 relationship between diffuse fraction and total SW, and which require fuller investigation for future

612 emission reduction scenarios

613

614 One of the largest causes of uncertainty over future maize yields on the NCP is the interaction of PM and

615 ozone pollution. As PM pollution has decreased in the NCP, ozone pollution has increased (Zeng *et al.*,

616 2019), and while this principally reflects a reduction in NO_x emissions, it has also been partly attributed to

617 increased light intensity increasing the rate of photochemical formation of ozone (Li *et al.*, 2019). Elevated

618 concentrations of ozone were estimated to have decreased maize yields across the USA by ~10%

619 between 1980 and 2011 (McGrath *et al.*, 2015). Yield gains from reductions in PM pollution in the NCP

620 may therefore be offset or outweighed by losses due to rising ozone concentrations, and it will be critical

621 to determine how the two interact. It is imperative that future emissions reduction strategies address PM

622 and ozone pollution together.

5. Funding Sources

6. References

Alton, P. B. (2008). Reduced carbon sequestration in terrestrial ecosystems under overcast skies compared to clear skies. *Agricultural and Forest Meteorology*, *148*(10), 1641–1653. https://doi.org/10.1016/J.AGRFORMET.2008.05.014

ALTON, P. B., NORTH, P. R., & LOS, S. O. (2007). The impact of diffuse sunlight on canopy light-use efficiency, gross photosynthetic product and net ecosystem exchange in three forest biomes. *Global Change Biology*, *13*(4), 776–787. https://doi.org/10.1111/j.1365-2486.2007.01316.x

An, Z., Huang, R. J., Zhang, R., Tie, X., Li, G., Cao, J., … Ji, Y. (2019). Severe haze in northern China: A synergy of anthropogenic emissions and atmospheric processes. *Proceedings of the National Academy of Sciences of the United States of America*. https://doi.org/10.1073/pnas.1900125116

Aziz, R. M., Zabawi, A. G. M., Azdawiyah, A. T. S., & Fazlyzan, A. (2019). Effects of haze on net photosynthetic rate , stomatal conductance and yield of Malaysian rice (Oryza sativa L .) varieties. *Journal of Agricultural and Food Science*, *47*(1), 1–13.

Best, M. J., Pryor, M., Clark, D. B., Rooney, G. G., Essery, R. . L. H., Ménard, C. B., … Harding, R. J. (2011). The Joint UK Land Environment Simulator (JULES), model description – Part 1: Energy and water fluxes. *Geoscientific Model Development*, *4*(3), 677–699. https://doi.org/10.5194/gmd-4-677-2011

Boman, J., Shaltout, A. A., Abozied, A. M., & Hassan, S. K. (2013). On the elemental composition of $PM_{2.5}$ in central Cairo, Egypt. *X-Ray Spectrometry*, *42*(4), 276–283. https://doi.org/10.1002/xrs.2464

648   Brodersen, C. R., & Vogelmann, T. C. (2010). Do changes in light direction affect absorption profiles

649   in leaves? *Functional Plant Biology*, *37*(5), 403. https://doi.org/10.1071/FP09262

650   Burney, J., & Ramanathan, V. (2014). Recent climate and air pollution impacts on Indian agriculture.

651   *Proceedings of the National Academy of Sciences of the United States of America*, *111*(46), 16319–

652   16324. https://doi.org/10.1073/pnas.1317275111

653   Chameides, W. L., Yu, H., Liu, S. C., Bergin, M., Zhou, X., Mearns, L., … Giorgi, F. (1999). Case

654   study of the effects of atmospheric aerosols and regional haze on agriculture: An opportunity to

655   enhance crop yields in China through emission controls? *Proceedings of the National Academy of*

656   *Sciences of the United States of America*. https://doi.org/10.1073/pnas.96.24.13626

657   Chen, H., Wang, H., 2015. Haze days in North China and the associated atmospheric circulations

658   based on daily visibility data from 1960 to 2012. J. Geophys. Res.

659   https://doi.org/10.1002/2015JD023225Cheng, Z., Wang, S., Jiang, J., Fu, Q., Chen, C., Xu, B., …

660   Hao, J. (2013). Long-term trend of haze pollution and impact of particulate matter in the Yangtze

661   River Delta, China. *Environmental Pollution*. https://doi.org/10.1016/j.envpol.2013.06.043

662   Cheng, S. J., Bohrer, G., Steiner, A. L., Hollinger, D. Y., Suyker, A., Phillips, R. P., & Nadelhoffer, K.

663   J. (2015). Variations in the influence of diffuse light on gross primary productivity in temperate

664   ecosystems. *Agricultural and Forest Meteorology*, *201*, 98–110.

665   https://doi.org/10.1016/J.AGRFORMET.2014.11.002

666   China: Air Quality Standards | Transport Policy. (2013). Retrieved May 18, 2020, from

667   https://www.transportpolicy.net/standard/china-air-quality-standards/

668   Clark, D. B., Mercado, L. M., Sitch, S., Jones, C. D., Gedney, N., Best, M. J., … Cox, P. M. (2011).

669   The Joint UK Land Environment Simulator (JULES), Model description – Part 2: Carbon fluxes and

670   vegetation. *Geoscientific Model Development Discussions*, *4*(1), 641–688.

671   https://doi.org/10.5194/gmdd-4-641-2011

672   Cohan, D. S., Xu, J., Greenwald, R., Bergin, M. H., & Chameides, W. L. (2002). Impact of

673   atmospheric aerosol light scattering and absorption on terrestrial net primary productivity. *Global*

674   *Biogeochemical Cycles*, *16*(4), 37-1-37–12. https://doi.org/10.1029/2001GB001441

675   Copernicus Climate Change Service (C3S). (2017). ERA5: Fifth generation of ECMWF atmospheric

676   reanalyses of the global climate . Copernicus Climate Change Service Climate Data Store (CDS).

677   Dhillon, B. S., Kataria, P., & Dhillon, P. K. (2010). *National food security vis-à-vis sustainability of*

678   *agriculture in high crop productivity regions*. CURRENT SCIENCE (Vol. 98).

679   Dohleman, F.G., Long, S.P., 2009. More productive than maize in the Midwest: How does

680   Miscanthus do it? Plant Physiol. https://doi.org/10.1104/pp.109.139162

681   FAOSTAT. (n.d.-a). Retrieved April 2, 2020, from

682   http://www.fao.org/giews/countrybrief/country.jsp?code=CHN

683   FAOSTAT. (n.d.-b). FAOSTAT Crop Database. Retrieved November 30, 2018, from

684   http://www.fao.org/faostat/en/#data/QC

685   FAOSTAT. (n.d.-c. FAOSTAT Crop Database. Retrieved September, 2020, from

686   http://www.fao.org/faostat/en/#data/QC

687   Feng, Z., Hu, E., Wang, X., Jiang, L., Liu, X., 2015. Ground-level O 3 pollution and its impacts on

688   food crops in China : A review. Environ. Pollut. 199, 42–48.

689   https://doi.org/10.1016/j.envpol.2015.01.016

690   Gao, Y., Zhang, M., Liu, Z., Wang, L., Wang, P., Xia, X., … Zhu, L. (2015). Modeling the feedback

691   between aerosol and meteorological variables in the atmospheric boundary layer during a severe

692   fog-haze event over the North China Plain. *Atmospheric Chemistry and Physics*.

693   https://doi.org/10.5194/acp-15-4279-2015

694   Gorai, A.K., Tchounwou, P.B., Biswal, S.S., Tuluri, F., 2018. Spatio-Temporal Variation of

695   Particulate Matter(PM2.5) Concentrations and Its Health Impacts in a Mega City, Delhi in India.

696   Environ. Health Insights 12. https://doi.org/10.1177/1178630218792861

697   Government, M. of E. and F. (2012). Energy Statistics. *China Statistical Yearbook*.

698   https://doi.org/Twenty first issue

699   Greenwald, R., Bergin, M. H., Xu, J., Cohan, D., Hoogenboom, G., & Chameides, W. L. (2006). The

700   influence of aerosols on crop production: A study using the CERES crop model. *Agricultural*

701   *Systems*. https://doi.org/10.1016/j.agsy.2005.10.004

702   Gu, L., Baldocchi, D., Verma, S. B., Black, T. A., Vesala, T., Falge, E. M., & Dowty, P. R. (2002).

703   Advantages of diffuse radiation for terrestrial ecosystem productivity. *Journal of Geophysical*

704   *Research Atmospheres*, *107*(5–6), ACL 2-1. https://doi.org/10.1029/2001jd001242

705   Guo, S., Hu, M., Zamora, M. L., Peng, J., Shang, D., Zheng, J., … Zhang, R. (2014).

706   *l Change Biology*, *24*(3), 987–1000. https://doi.org/10.1111/gcb.13898

707   Han, S., Bian, H., Zhang, Y., Wu, J., Wang, Y., Tie, X., … Yao, Q. (2012). Effect of aerosols on

708   visibility and radiation in spring 2009 in Tianjin, China. *Aerosol and Air Quality Research*.

709   https://doi.org/10.4209/aaqr.2011.05.0073

710   Hu, X., & Zimmer, Y. (2013). *China´s Corn Production*.

711   Hua, Y., Cheng, Z., Wang, S., Jiang, J., Chen, D., Cai, S., … Yu, J. (2015). Characteristics and

712   source apportionment of PM2.5 during a fall heavy haze episode in the Yangtze River Delta of

713   China. *Atmospheric Environment*. https://doi.org/10.1016/j.atmosenv.2015.03.046

714   Huang, K., Wang, S., Zhou, L., Wang, H., Zhang, J., Yan, J., … Shi, P. (2014). Impacts of Diffuse

715   Radiation on Light Use Efficiency across Terrestrial Ecosystems Based on Eddy Covariance

716   Observation in China. *PLoS ONE*, *9*(11), e110988. https://doi.org/10.1371/journal.pone.0110988

717   Huang, R.-J., Zhang, Y., Bozzetti, C., Ho, K.-F., Cao, J.-J., Han, Y., … Prévôt, A. S. H. (2014). High

718   secondary aerosol contribution to particulate pollution during haze events in China. *Nature*,

719   *514*(7521), 218–222. https://doi.org/10.1038/nature13774

720   Jain, S.L., Arya, B.C., Kumar, A., Ghude, S.D., Kulkarni, P.S., 2005. Observational study of surface

721   ozone at New Delhi, India. Int. J. Remote Sens. https://doi.org/10.1080/01431160500076616

722   Jiang, H., Yang, Y., Wang, H., Bai, Y., & Bai, Y. (2020). Surface diffuse solar radiation determined

723   by reanalysis and satellite over East Asia: Evaluation and comparison. *Remote Sensing*.

724   https://doi.org/10.3390/RS12091387

725   Just, A. C., Wright, R. O., Schwartz, J., Coull, B. A., Baccarelli, A. A., Tellez-Rojo, M. M., … Kloog, I.

726   (2015). Using High-Resolution Satellite Aerosol Optical Depth To Estimate Daily PM2.5

727   Geographical Distribution in Mexico City. *Environmental Science & Technology*, *49*(14), 8576–8584.

728   https://doi.org/10.1021/acs.est.5b00859

729   Kanniah, K. D., Beringer, J., North, P., & Hutley, L. (2012). Control of atmospheric particles on

730   diffuse radiation and terrestrial plant productivity: A review. *Progress in Physical Geography*.

731   https://doi.org/10.1177/0309133311434244

732   Karanasiou, A., Querol, X., Alastuey, A., Perez, N., Pey, J., Perrino, C., … Pascal, M. (2014).

733   Particulate matter and gaseous pollutants in the Mediterranean Basin: Results from the MED-

734   PARTICLES project. *Science of the Total Environment*.

735   https://doi.org/10.1016/j.scitotenv.2014.04.096

736   Kimball, B. A., Boote, K. J., Hatfield, J. L., Ahuja, L. R., Stockle, C., Archontoulis, S., … Williams, K.

737   (2019). Simulation of maize evapotranspiration: An inter-comparison among 29 maize models.

738   *Agricultural and Forest Meteorology*. https://doi.org/10.1016/j.agrformet.2019.02.037

739   Khoder, M.I., 2009. Diurnal, seasonal and weekdays-weekends variations of ground level ozone

740   concentrations in an urban area in greater Cairo. Environ. Monit. Assess.

741   https://doi.org/10.1007/s10661-008-0208-7

742   Kuhlmann, J., & Quaas, J. (2010). How can aerosols affect the Asian summer monsoon?

743   Assessment during three consecutive pre-monsoon seasons from CALIPSO satellite data.

744   *Atmospheric Chemistry and Physics*. https://doi.org/10.5194/acp-10-4673-2010

745   LEI, H.-M., & YANG, D.-W. (2009). Seasonal and interannual variations in carbon dioxide exchange

746   over a cropland in the North China Plain. *Global Change Biology*, *16*(11), no-no.

747   https://doi.org/10.1111/j.1365-2486.2009.02136.x

748   Li, H., Jiang, D., Wollenweber, B., Dai, T., & Cao, W. (2010). Effects of shading on morphology,

749   physiology and grain yield of winter wheat. *European Journal of Agronomy*, *33*(4), 267–275.

750   https://doi.org/10.1016/J.EJA.2010.07.002

751   Li, J. (2009). Production, Breeding and Process of Maize in China. In *Handbook of Maize: Its*

752   *Biology* (pp. 563–576). Springer New York. https://doi.org/10.1007/978-0-387-79418-1_28

753   Li, K., Jacob, D. J., Liao, H., Shen, L., Zhang, Q., & Bates, K. H. (2019). Anthropogenic drivers of

754   2013–2017 trends in summer surface ozone in China. *Proceedings of the National Academy of*

755   *Sciences of the United States of America*. https://doi.org/10.1073/pnas.1812168116

756   Li, T., & Yang, Q. (2015). Advantages of diffuse light for horticultural production and perspectives for

757   further research. *Frontiers in Plant Science*, *6*, 704. https://doi.org/10.3389/fpls.2015.00704

758   Liu, Y., Wang, E., Yang, X., & Wang, J. (2010). Contributions of climatic and crop varietal changes

759   to crop production in the North China Plain, since 1980s. *Global Change Biology*, *16*(8), 2287–2299.

760   https://doi.org/10.1111/j.1365-2486.2009.02077.x

761   Masutomi, Y., Kinose, Y., Takimoto, T., Yonekura, T., Oue, H., Kobayashi, K., 2018. Ozone

762   changes the linear relationship between photosynthesis and stomatal conductance and decreases

763   water use efficiency in rice. Sci. Total Environ. https://doi.org/10.1016/J.SCITOTENV.2018.11.132

764   Mcgrath, J. M., Betzelberger, A. M., Wang, S., Shook, E., Zhu, X., & Long, S. P. (2015). An analysis

765   of ozone damage to historical maize and soybean yields in the United States.

766   https://doi.org/10.1073/pnas.1509777112

767   Mercado, L. M., Bellouin, N., Sitch, S., Boucher, O., Huntingford, C., Wild, M., & Cox, P. M. (2009).

768   Impact of changes in diffuse radiation on the global land carbon sink. *Nature*, *458*(7241), 1014–

769   1017. https://doi.org/10.1038/nature07949

770   Mina, U., Chandrashekara, T. K., Kumar, S. N., Meena, M. C., Yadav, S., Tiwari, S., … Kumar, R.

771   (2018a). Impact of particulate matter on basmati rice varieties grown in Indo-Gangetic Plains of

772   India: Growth, biochemical, physiological and yield attributes. *Atmospheric Environment*, *188*, 174–

773   184. https://doi.org/10.1016/J.ATMOSENV.2018.06.015

774   Mina, U., Chandrashekara, T. K., Kumar, S. N., Meena, M. C., Yadav, S., Tiwari, S., … Kumar, R.

775   (2018b). Impact of particulate matter on basmati rice varieties grown in Indo-Gangetic Plains of

776   India: Growth, biochemical, physiological and yield attributes. *Atmospheric Environment*, *188*, 174–

777   184. https://doi.org/10.1016/j.atmosenv.2018.06.015

778   Climate and the efficiency of crop production in Britain, 1977. . Philos. Trans. R. Soc. London. B,

779   Biol. Sci. https://doi.org/10.1098/rstb.1977.0140

780   Moosmüller, H., Chakrabarty, R. K., & Arnott, W. P. (2009, July 1). Aerosol light absorption and its

781   measurement: A review. *Journal of Quantitative Spectroscopy and Radiative Transfer*. Pergamon.

782   https://doi.org/10.1016/j.jqsrt.2009.02.035

783   Niyogi, D., Chang, H., Saxena, V. K., Holt, T., Alapaty, K., Booker, F., … Xue, Y. (2004). Direct

784   observations of the effects of aerosol loading on net ecosystem CO_2 exchanges over different

785   landscapes. *Geophysical Research Letters*, *31*(20), L20506. https://doi.org/10.1029/2004GL020915

786   Ojha, N., Sharma, A., Kumar, M., Girach, I., Ansari, T. U., Sharma, S. K., … Gunthe, S. S. (2020).

787   On the widespread enhancement in fine particulate matter across the Indo-Gangetic Plain towards

788   winter. *Scientific Reports*, *10*(1), 1–9. https://doi.org/10.1038/s41598-020-62710-8

789   Ort, D.R., Merchant, S.S., Alric, J., Barkan, A., Blankenship, R.E., Bock, R., Croce, R., Hanson,

790   M.R., Hibberd, J.M., Long, S.P., Moore, T.A., Moroney, J., Niyogi, K.K., Parry, M.A.J., Peralta-

791   Yahya, P.P., Prince, R.C., Redding, K.E., Spalding, M.H., Van Wijk, K.J., Vermaas, W.F.J., Von

792   Caemmerer, S., Weber, A.P.M., Yeates, T.O., Yuan, J.S., Zhu, X.G., 2015. Redesigning

793   photosynthesis to sustainably meet global food and bioenergy demand. Proc. Natl. Acad. Sci. U. S.

794   A. https://doi.org/10.1073/pnas.1424031112

795   Osborne, T., Gornall, J., Hooker, J., Williams, K., Wiltshire, A., Betts, R., & Wheeler, T. (2015).

796   JULES-crop: a parametrisation of crops in the Joint UK Land Environment Simulator. *Geoscientific*

797   *Model Development*, *8*(4), 1139–1155. https://doi.org/10.5194/gmd-8-1139-2015

798   Peltier, R. E., Cromar, K. R., Ma, Y., Fan, Z. H., & Lippmann, M. (2011). Spatial and seasonal

799   distribution of aerosol chemical components in New York City: (2) Road dust and other tracers of

800   traffic-generated air pollution. *Journal of Exposure Science and Environmental Epidemiology*.

801   https://doi.org/10.1038/jes.2011.15

802   Proctor, J., Hsiang, S., Burney, J., Burke, M., & Schlenker, W. (2018). Estimating global agricultural

effects of geoengineering using volcanic eruptions. *Nature*, *560*(7719), 480–483. https://doi.org/10.1038/s41586-018-0417-3

Qin, K., Zou, J., Guo, J., Lu, M., Bilal, M., Zhang, K., … Zhang, Y. (2018). Estimating PM1 concentrations from MODIS over Yangtze River Delta of China during 2014–2017. *Atmospheric Environment*, *195*, 149–158. https://doi.org/10.1016/J.ATMOSENV.2018.09.054

Qu, W., Wang, J., Zhang, X., Sheng, L., & Wang, W. (2016). Opposite seasonality of the aerosol optical depth and the surface particulate matter concentration over the north China Plain. *Atmospheric Environment*, *127*, 90–99. https://doi.org/10.1016/j.atmosenv.2015.11.061

Quan, J., Zhang, Q., He, H., Liu, J., Huang, M., & Jin, H. (2011). Analysis of the formation of fog and haze in North China Plain (NCP). *Atmospheric Chemistry and Physics*. https://doi.org/10.5194/acp-11-8205-2011

Ramanathan, V., Crutzen, P. J., Kiehl, J. T., & Rosenfeld, D. (2001). Atmosphere: Aerosols, climate, and the hydrological cycle. *Science*. https://doi.org/10.1126/science.1064034

Rap, A., Scott, C. E., Reddington, C. L., Mercado, L., Ellis, R. J., Garraway, S., … Spracklen, D. V. (2018). Enhanced global primary production by biogenic aerosol via diffuse radiation fertilization. *Nature Geoscience*, *11*(9), 640–644. https://doi.org/10.1038/s41561-018-0208-3

Rap, A., Spracklen, D. V., Mercado, L., Reddington, C. L., Haywood, J. M., Ellis, R. J., … Butt, N. (2015). Fires increase Amazon forest productivity through increases in diffuse radiation. *Geophysical Research Letters*, *42*(11), 4654–4662. https://doi.org/10.1002/2015GL063719

Roderick, M. L., Farquhar, G. D., Berry, S. L., & Noble, I. R. (2001a). On the direct effect of clouds and atmospheric particles on the productivity and structure of vegetation. *Oecologia*, *129*(1), 21–30. https://doi.org/10.1007/s004420100760

Roderick, M. L., Farquhar, G. D., Berry, S. L., & Noble, I. R. (2001b). On the direct effect of clouds and atmospheric particles on the productivity and structure of vegetation, 21–30. https://doi.org/10.1007/s004420100760

828   Sacks, W. J., Deryng, D., Foley, J. A., & Ramankutty, N. (2010). Crop planting dates: An analysis of

829   global patterns. *Global Ecology and Biogeography*. https://doi.org/10.1111/j.1466-

830   8238.2010.00551.x

831   Santurtún, A., González-Hidalgo, J.C., Sanchez-Lorenzo, A., Zarrabeitia, M.T., 2015. Surface ozone

832   concentration trends and its relationship with weather types in Spain (2001-2010). Atmos. Environ.

833   https://doi.org/10.1016/j.atmosenv.2014.11.005

834   Shen, R., Schäfer, K., Schnelle-Kreis, J., Shao, L., Norra, S., Kramar, U., … Emeis, S. (2018).

835   Seasonal variability and source distribution of haze particles from a continuous one-year study in

836   Beijing. *Atmospheric Pollution Research*. https://doi.org/10.1016/j.apr.2017.12.013

837   Shihuang, Z., & Kaijian, H. (2010). Maize and the formal agricultural research and development

838   system: evolution, challenges and alternatives. In *Seeds and Synergies* (pp. 13–28). Practical

839   Action Publishing. https://doi.org/10.3362/9781780440330.002

840   Shmool, J.L.C., Kinnee, E., Sheffield, P.E., Cloughterty, J.E., 2016. Spatio-temporal ozone variation

841   in a case-crossover analysis of childhood asthma hospital visits in New York City. Environ. Res.

842   https://doi.org/10.1016/j.envres.2016.01.020

843   Strada, S., Unger, N., & Yue, X. (2015). Observed aerosol-induced radiative effect on plant

844   productivity in the eastern United States. *Atmospheric Environment*, *122*, 463–476.

845   https://doi.org/10.1016/j.atmosenv.2015.09.051

846   Timsina, J. (2012). *Review of rice-wheat in IGP- Advances in Agronomy* (Vol. 117). Elsevier Inc.

847   Retrieved from https://www.academia.edu/9776292/Review_of_rice-wheat_in_IGP-

848   _Advances_in_Agronomy

849   Urraca, R., Huld, T., Gracia-Amillo, A., Martinez-de-Pison, F. J., Kaspar, F., & Sanz-Garcia, A.

850   (2018). Evaluation of global horizontal irradiance estimates from ERA5 and COSMO-REA6

851   reanalyses using ground and satellite-based data. *Solar Energy*, *164*, 339–354.

852   https://doi.org/10.1016/j.solener.2018.02.059

853   van Donkelaar, A., Martin, R. V., Spurr, R. J. D., Drury, E., Remer, L. A., Levy, R. C., & Wang, J.

854   (2013). Optimal estimation for global ground-level fine particulate matter concentrations. *Journal of*

855   *Geophysical Research: Atmospheres*, *118*(11), 5621–5636. https://doi.org/10.1002/jgrd.50479

856   Wang, H., Tian, M., Li, X., Chang, Q., Cao, J., Yang, F., … He, K. (2015). Chemical Composition

857   and Light Extinction Contribution of PM2.5 in Urban Beijing for a 1-Year Period. *Aerosol and Air*

858   *Quality Research*, *15*(6), 2200–2211. https://doi.org/10.4209/aaqr.2015.04.0257

859   WHO. (2015). WHO | Ambient (outdoor) air quality and health. Retrieved from

860   https://web.archive.org/web/20160104165807/http://www.who.int/mediacentre/factsheets/fs313/en/

861   Wickens, G. E., & Horn, H. S. (1972). The Adaptive Geometry of Trees. *Kew Bulletin*.

862   https://doi.org/10.2307/4109478

863   Williams, K., Gornall, J., Harper, A., Wiltshire, A., Hemming, D., Quaife, T., … Scoby, D. (2017).

864   Evaluation of JULES-crop performance against site observations of irrigated maize from Mead,

865   Nebraska. *Geoscientific Model Development*, *10*(3), 1291–1320. https://doi.org/10.5194/gmd-10-

866   1291-2017

867   Xie, X., Wang, T., Yue, X., Li, S., Zhuang, B., & Wang, M. (2020). Effects of atmospheric aerosols

868   on terrestrial carbon fluxes and CO2 concentrations in China. *Atmospheric Research*, *237*, 104859.

869   https://doi.org/10.1016/J.ATMOSRES.2020.104859

870   Yang, S., Duan, F., Ma, Y., Li, H., Ma, T., Zhu, L., … He, K. (2020). Mixed and intensive haze

871   pollution during the transition period between autumn and winter in Beijing, China. *Science of the*

872   *Total Environment*. https://doi.org/10.1016/j.scitotenv.2019.134745

873   Yang, X., Jiang, L., Zhao, Wenji, Xiong, Q., Zhao, Wenhui, Yan, X., 2018. Comparison of ground-

874   based PM2.5 and PM10 concentrations in China, India, and the U.S. Int. J. Environ. Res. Public

875   Health. https://doi.org/10.3390/ijerph15071382

876   Yao, L., Yang, L., Yuan, Q., Yan, C., Dong, C., Meng, C., … Wang, W. (2016). Sources

877   apportionment of PM2.5 in a background site in the North China Plain. Science of the Total

878   Environment. https://doi.org/10.1016/j.scitotenv.2015.09.123

879   Liu, Y., Wang, E., Yang, X., Wang, J., 2010. Contributions of climatic and crop varietal changes to

880   crop production in the North China Plain, since 1980s. Glob. Chang. Biol. 16, 2287–2299.

881   https://doi.org/10.1111/j.1365-2486.2009.02077.x

882   Yue, X., & Unger, N. (2017). Aerosol optical depth thresholds as a tool to assess diffuse radiation

883   fertilization of the land carbon uptake in China. *Atmospheric Chemistry and Physics*, *17*(2), 1329–

884   1342. https://doi.org/10.5194/acp-17-1329-2017

885   Zeng, Y., Cao, Y., Qiao, X., Seyler, B. C., & Tang, Y. (2019). Air pollution reduction in China: Recent

886   success but great challenge for the future. *Science of the Total Environment*.

887   https://doi.org/10.1016/j.scitotenv.2019.01.262

888   Zhai, S., Jacob, D. J., Wang, X., Shen, L., Li, K., Zhang, Y., … Liao, H. (2019). Fine particulate

889   matter (PM2.5) trends in China, 2013-2018. separating contributions from anthropogenic emissions

890   and meteorology. *Atmospheric Chemistry and Physics*. https://doi.org/10.5194/acp-19-11031-2019

891   Zhao, L., Wang, W., Hao, T., Qu, W., Sheng, L., Luo, C., … Zhou, Y. (2020). The autumn haze-fog

892   episode enhanced by the transport of dust aerosols in the Tianjin area. *Atmospheric Environment*.

893   https://doi.org/10.1016/j.atmosenv.2020.117669

894   Zhou, Li, Chen, X., & Tian, X. (2018). The impact of fine particulate matter (PM2.5) on China's

895   agricultural production from 2001 to 2010. *Journal of Cleaner Production*, *178*, 133–141.

896   https://doi.org/10.1016/J.JCLEPRO.2017.12.204

897   Zhou, Luxi, Schwede, D. B., Wyat Appel, K., Mangiante, M. J., Wong, D. C., Napelenok, S. L., …

898   Zhang, B. (2019). The impact of air pollutant deposition on solar energy system efficiency: An

899   approach to estimate PV soiling effects with the Community Multiscale Air Quality (CMAQ) model.

900   *Science of The Total Environment*, *651*, 456–465.

901   https://doi.org/10.1016/J.SCITOTENV.2018.09.194

902   Zhu, X.G., Long, S.P., Ort, D.R., (2010) Improving Photosynthetic Efficiency for Greater Yield.

903   Annual Review of Plant Biology, 61, 235-261.

904   Zhu, Z., Sun, X., Zhao, F., & Meixner, F. X. (2015). ScienceDirect Ozone concentrations , flux and

905   potential effect on yield during wheat growth in the Northwest-Shandong Plain of China. *JES*, *34*, 1–

906   9. https://doi.org/10.1016/j.jes.2014.12.022